ACS OMEGA

http://pubs.acs.org/journal/acsodf

Article

Experimental Study on the Basic Properties of a Green New Coal Mine Grouting Reinforcement Material

Xianxiang Zhu, Qi Zhang,* Wenquan Zhang,* Jianli Shao, Zaiyong Wang, and Xintao Wu

Cite This: *ACS Omega* 2020, 5, 16722−16732

Read Online

ACCESS | Metrics & More | Article Recommendations

ABSTRACT: Waste tires are internationally recognized as hazardous waste. Many waste tires storing in the open air for a long time will not only waste the land resources but also pollute the environment after the incineration. Meanwhile, the cumulative accumulation of fly ash in China has also been one of the largest sources of solid waste in coal mines. Under the action of high winds, the accumulated fly ash forms flying dust, which pollutes the environment and endangers human health. Herein, a new type of grouting material for floor reinforcement was developed based on solid waste products using the waste tire rubber particles and fly ash. Using this new material, disaster accidents such as flooding and casualties caused by the inrush of the floor-confined water due to floor fractures, activation, and expansion in the mining process can be greatly reduced, thereby ensuring the safety of coal mine production. The grout body was prepared using a large amount of fly ash, waste tire rubber particles and clay, and mixing additives. The ratio optimization test, uniaxial compressive strength test, permeability characteristic test, stability test, and microanalysis of mine water environment were performed. From the test results, the macrophysical and chemical properties including optimal mix ratio, compressive strength, permeability coefficient, and stability of mine water environment were obtained. The microstructural properties of the grouts were analyzed using scanning electron microscopy microanalysis methods. Considering the situation of the coal floor and attempting to use as many solid waste products as possible, the optimized proportion that can meet the requirements of low cost, high bonds, and dense filling is as follows: 20% of rubber particles, 65% of fly ash, 15% of clay, and 1% of nanosilica. Furthermore, this study can provide scientific reference for large-scale floor grouting reinforcement and large-scale utilization of solid waste products.

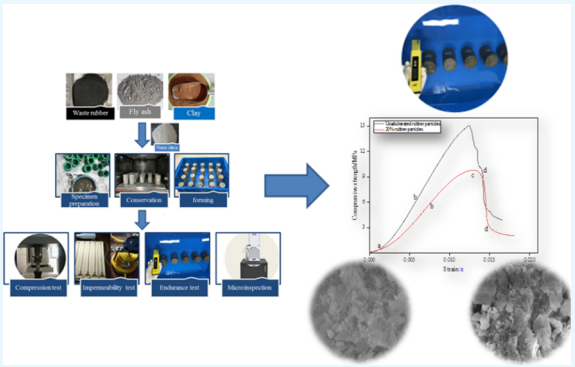

1. INTRODUCTION

With the continuous development of China's economy, the use of automobiles has greatly been extended in people's lives. Consequently, automobiles have also caused huge pollution. Until 2019, China's waste tires have reached 14.59 million tons. Most of these waste tires have simply been dumped in open air or landfill sites, which have caused a huge waste of resources and severe environmental pollution.[1−3] Fly ash is a solid waste generated in the power generation process of coal-fired power plants. Fly ash has a cumulative storage volume of 2 billion tons and a large annual total emission, thus becoming the largest industrial and mining solid waste source in China.[4−6] With the advancement of technology and the increasing awareness of environmental protection in various countries, many scholars have focused on the comprehensive utilization and the harmless treatment of solid waste products. The recycling of waste tires mainly includes high-temperature pyrolysis,[7] combustion reuse,[8] chemical refining,[9,10] making rubber particles and rubber powder,[11−13] and so forth. However, centralized incineration is used as the main treatment method in China, as shown in Figure 1.

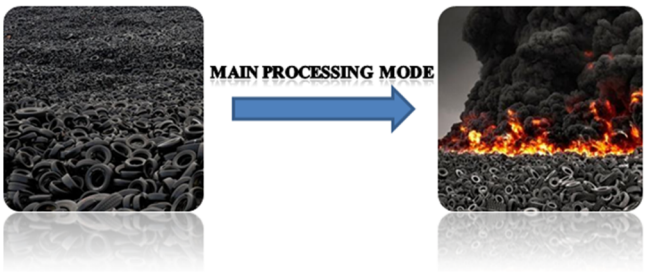

Figure 1. Waste tire disposal method.

Received: April 9, 2020
Accepted: June 5, 2020
Published: June 28, 2020

Since the 1990s, waste tire fragments have also been used as materials in landfill projects, drainage, leachate treatment, daily covering, and thermal insulation.[14−16] Previous studies have found that waste tire fragments or particles have better adsorption performance for organic pollutants. Meanwhile, tire particles can help improve the expansion and contraction properties of expansive soils.[17−19] Because waste tires have relatively stable physical and chemical properties, they have very large production yield and low cost in China. The researchers in China and other countries have started to investigate the use of waste rubber tires in geotechnical engineering.[20,21] Xin[22,23] investigated the relationship between the proportion and strength of lightweight concrete using waste tire rubber particles as lightweight materials. In addition, the effect of factors such as rubber particle content, cement content, water content, and curing age on the unconfined compressive strength of lightweight concrete as well as the effect of the content of rubber particles and cement on the shape of its stress−strain curve were analyzed. The variation law of the strength and deformation of the sample with the mix ratio of the concrete was obtained. Based on the particle flow theory and PFC2D program, Liu[24,25] established a biaxial compression test numerical model of rubber sand. Through the comprehensive comparison of the simulation results with the triaxial CD shear test of the indoor rubber sand, it was demonstrated that when the volume content of rubber particle was between 30 and 40%, the load-deformation capacity relationship was most stable. Feng[26] prepared two pyrolytic carbon blacks from waste tires. The thermal aging and photo-oxidative aging of PCB-modified asphalt were evaluated using the methods of melt blending, film furnace test, pressure aging container, and natural aging. Gupta[27] used waste tire rubber as a raw material to prepare a new type of carbon adsorbent (RTAC) through physical activation. The ability of RTAC to remove lead and nickel ions in water was studied, and the results revealed that a well-developed mesoporous structure was beneficial to enhance the batch adsorption capacity to remove the metal ions. Cazan[28] used waste tire rubber as a matrix, PET as a reinforcing material, HDPE as an additive, and ceramic powder as a low-content filler to synthesize the PET−rubber composite material. By changing the composition of the composite, the interface properties of tire rubber and PET were improved, and the effect of different oxidation fillers on the interfacial properties of PET−rubber composites was investigated. Li[29] used dynamic triaxial tests to study the effect of waste tire rubber particles on the dynamic strength, dynamic modulus, and shear strength of fly ash soil. The test results were compared with the dynamic characteristics of fly ash soil. The analysis proved that under the same confining pressure, the dynamic strength of the rubber particle−fly ash concrete decreased with the increase of the number of failure cycles. Under the same number of failure cycles, the dynamic strength of the sample increased with the increase of confining pressure. Aslani[30] replaced natural aggregates with waste rubber particles and lightweight volcanic slag and added microfibers in the synthesis process of concrete. Through laboratory tests, the characteristics of microfibers in mixed concrete and the performance of concrete at high temperatures were determined. Aly[31] developed a new geopolymer concrete using waste rubber particles as the aggregate mixed with steel slag or blast furnace slag. Waste rubber particles provided mixed concrete with high compressive strength, ductility, and impact resistance; therefore, the mixed concrete can be used as the structural element to withstand shock and dynamic loads. Presti[32] summarized the wet process to synthesize rubber asphalt mixture over the past 40 years, confirming that waste rubber particles have a good effect on road paving and performance improvement of pavement.

In addition, researchers in China and abroad have performed a large number of studies on the preparation of grouting materials using industrial and mining solid waste. Sun[33] analyzed the effects of solid mass concentration, the content ratio between fine vermiculite and fly ash on the workability and strength of the slurry backfill material. It was concluded that at a content of 15.67%, the fly ash had stronger activity, which can promote the early formation of calcium silicate gel and improve the strength of agglomerate formation of hydrated calcium silicate gel. Lee[34] determined the optimal synthesis conditions of zeolites synthesized from fly ash through considering the composition of fly ash, pretreatment procedures, and hydrothermal synthesis conditions (matrix composition and synthesis temperature/time). Chen[35] developed a new type of high-strength grouting material based on industrial waste-active fly ash. In view of the seepage problems in hydraulic and geotechnical engineering, Wan[36] analyzed the effect of fly ash content on the impermeability of cement water glass slurry. Through field tests, when the amount of fly ash was 25%, the impermeability can meet the specification requirements. Through experimental study, Zhang[37] developed a new type of grouting material with high strength and high impermeability using the fly ash with the content of 30% and some additives.

The application of waste rubber particles in geotechnical engineering has been widely studied. However, the existing studies are only limited to ground applications, while the application in the industrial and mining industry was rarely reported. Meanwhile, the storage and pollution of industrial and mining solid wastes need to be resolved. The use of fly ash has received increasing attention from scholars in China and other countries. Nowadays, the problem of grouting reinforcement of coal seam floor and instability of surrounding rock roadway has become more and more stringent.[38−40] Based on the studies by experts and scholars in China and other countries, the best solution is grouting reinforcement.[41,42] Using the waste rubber particles in combination with solid waste from industrial and mining enterprises to develop suitable grouting and strengthening material can not only reduce the production cost but also recycle the waste and reduce the impact of waste on the environment.

In this paper, based on the research studies in China and other countries, a new type of grouting material suitable for grouting and strengthening of the coal floor was developed using a large amount of fly ash, waste rubber particles, and clay, supplemented with additives. The physical and chemical properties of the new materials were evaluated by means of mechanical and physical tests, impermeability tests, and stability tests in the water environment of the mine. In addition, the microcharacteristics of the grouting materials were analyzed with scanning electron microscopy (SEM). From the aspects of physical and chemical properties and internal structure, the differences and advantages of the developed grouting materials and other grouting materials were analyzed in this paper, providing a new way for the corresponding mines to choose the floor grouting and sealing reinforcement materials.

https://dx.doi.org/10.1021/acsomega.0c01626
ACS Omega 2020, 5, 16722−16732

2. RESULTS AND DISCUSSION

2.1. Compressive Strength Characteristics of New Grouting Materials at Different Ratios. After the grouting material is injected into the cracks of the floor and solidified, as the mining depth gradually increases, it is necessary to ensure that the floor cracks are densely filled to resist the dynamic water pressure during preinrush, reduce the permeability of the floor cracks, and enhance the extension and the compressive modulus of the strengthened floor. This is the primary requirement for the developed grouting material. On the basis of meeting the engineering applicability, three materials were used, that is, waste rubber particles (R), clay (C), and fly ash (F), supplemented by nanosilica. Multiple groups of tests were designed to evaluate the strength of the grout during the curing age. Under different amounts of rubber particles and silica, controlling other variables, the compressive strength characteristics of the grout were analyzed.

2.1.1. Influence Law of Different Waste Rubber Particle Contents on the Strength of Test Block. The stress−strain relationship curves of the grout test blocks corresponding to different dosages of rubber particles are shown in Figure 2.

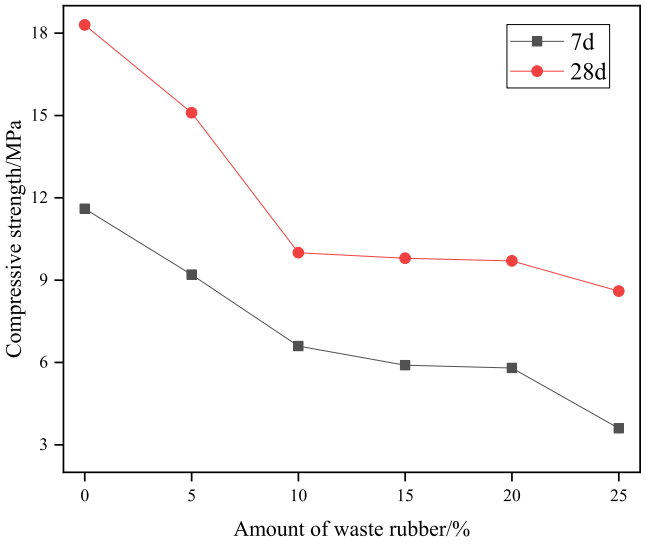

Figure 2. Uniaxial compressive strength of grouting stones with different amounts of rubber particles.

From Figure 2, it can be seen that when the rubber particle content was 0%, the grout exhibited the highest strength, which was 18.3 MPa at the age of 28 days. When the rubber particles were added instead of the aggregate, the strength of the grout was significantly reduced. When the rubber particles were mixed in the grout, they did not react with other materials but existed independently. Because of the special properties of the rubber particles, they exhibited strong elastic compression properties. When the rubber particle content was constantly changing, the strength of the grout changed significantly; that is, as the rubber particle content increased, the strength of the grout decreased, and the grout was exposed to larger compression and shear forces. When the amount of rubber particles was increased from 10 to 15 and 20%, the corresponding compressive strength decreased slowly with the increase of the amount of rubber particles. This phenomenon can be explained as follows: when the amount of rubber particles was increased within a certain range, the internal structural pores were small and uniformly arranged, and the rubber particles had a high degree of adhesion to other cementitious materials. In this case, the incorporation of certain rubber particles can cause the internal structure of the grout to be dense and thus slowly decrease the compressive strength of the grout. When the particle content exceeded 25%, the rubber particles were unevenly distributed in the grout, the spacing between the particles was reduced, and the combined effect of soil and water was affected. In this case, the bonding ability between the rubber particles and the soil was reduced, and the particles can easily peel off. As a result, the cement cannot withstand large pressure and shear force.

2.1.2. Influence Law of Different Nanosilica Content on the Strength of Test Block. It can be seen from Figure 3 that

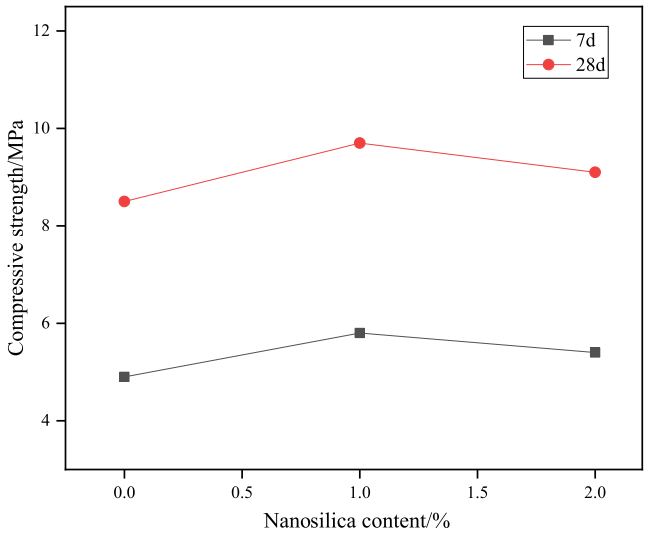

Figure 3. Uniaxial compressive strength changes of nanosilica contents of 0, 1, and 2%.

the compressive strength of the new material grout changes with the incorporation of nanosilica. As the amount of nanosilica increased, the strength of the grout first increased and then decreased. When the water−cement ratio was constant, the early-stage strength of the grout specimens with different clay contents did not have obvious variations. As the amount of nanosilica increased, the strength of the grout first increased and then decreased. Nanosilica can quickly undergo hydration reaction in a short period of time. The nanosilica actively reacted with the hydration products of fly ash and improved the early-stage strength of the grout. The internal structure of SiO_2 and Al_2O_3 in the fly ash was broken, and the activity of the fly ash was exciting. Then, the SiO_2 and Al_2O_3 in the fly ash can chemically react with the hydration product $Ca(OH)_2$ of the activator to generate gelled materials such as hydrated calcium silicate, calcium hydrated aluminate, and calcium hydrated aluminosilicate. Nanosilica reacted with the gelled material again to produce C−S−H gel, which wrapped around the fly ash and filled the microporous structure in the porosity wall of the hardened slurry, thus improving the compactness of the hardened slurry and increasing the strength of the grout. When the content of nanosilica was 1%, it can not only improve the workability of the grouting material but also benefit the strength development of the stomata wall of the grout. When the content of nanosilica was higher than 1% and continued to increase, the strength of the grout started to decrease.

https://dx.doi.org/10.1021/acsomega.0c01626
ACS Omega 2020, 5, 16722−16732

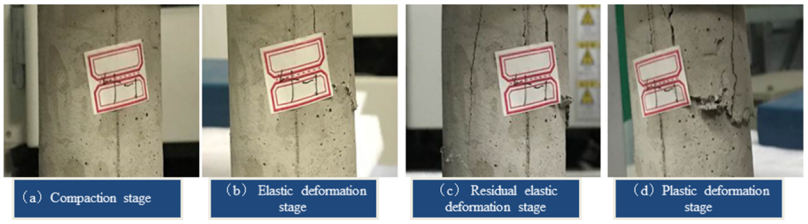

Figure 4. Test condition of compressive strength of grouting stone body when the content of rubber particles is 20%.

2.1.3. Stress−Strain Relationship of Grouting Consolidation. Figures 4 and 5 show the strength test results of the test

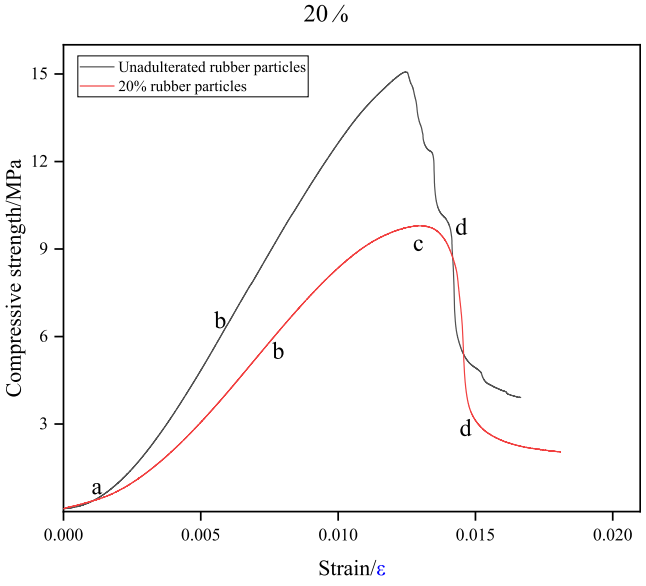

Figure 5. Stress−strain relationship curve.

blocks with the contents of rubber particles of 0 and 20%, the content of nanosilica of 1%, and the age of 28 days. The variation can basically be divided into four stages. The first stage was the fully compacted stage. Because of the uneven pores in the grout, the contact interface with the indenter was not closely fit. In the initial contact period, the distribution of the stress on the interface gradually became uniform with the increase of the load. The second stage was the elastic deformation stage. At this stage, the test block mainly underwent elastic deformation; that is, the indenter and the test block were in close contact, and the stress and strain had a positive linear relationship. The slope of this section in the stress−strain curve was the elastic modulus of the test block. From Figure 5, it can be seen that the slope of the stress−strain curve of the sample with 20% waste rubber particles was significantly smaller than that of the sample without rubber particles, which indicated that the addition of rubber particles reduced the elastic modulus of the grout. As a result, the elastic deformation of the grout was larger and the flexibility was increased. Therefore, this stage was the main rising section of the stress−strain curve. The third stage was the residual elastic deformation stage. At this stage, cracks began to appear on the surface of the grout, but overall, there was no significant deformation. This is because the rubber particles inside the test block can reduce the elastic modulus, and the test block can withstand large deformation, which reduces the stress concentration in the rock layer with grouting flow and maintain the effective strength of the grouting floor. Accordingly, the sealing and strengthening effect of the grout achieved the optimal state, and the strength of the grout gradually declined at this stage. The fourth stage was the plastic deformation stage. At this stage, large through cracks started to appear on the surface of the grout, and the axial stress began to decrease. Meanwhile, the plastic deformation of the grout began to increase rapidly, causing the stress to decrease.

2.2. Impermeability of Grouting Consolidation of the New Grouting Material. There are many methods for testing the permeability characteristics of the grout. In laboratory tests, triaxial permeability tests and conventional permeability tests have been commonly used.[43] In the conventional permeability test, a homogeneous sample at a specific dry density was prepared by a compaction test, and then, the permeability coefficient of the test piece at the corresponding dry density was calculated. The reliability of the test result using the conventional permeability test was relatively high. The conventional permeability test can be divided into two types, in which the constant head permeability test was normally used for the grout with large permeability ($k > 10^{-3}$ cm/s), while the variable head permeability test was used for the composite grout with a low permeability[44] ($k < 10^{-3}$ cm/s). In this paper, the impermeability characteristics of the grout were characterized by two measured parameters, that is, the impermeability coefficient and osmotic pressure. The permeability coefficient was measured by a TST-55 model permeameter. The osmotic pressure was measured by a SS-1.5 mortar permeameter. The variable head permeability coefficient is calculated as follows

$$K_T = 2.3\frac{aL}{A(t_2 - t_1)}\log\frac{H_1}{H_2} \quad (1)$$

where A is the cross-sectional area of the head pipe (cm^2), a is the sample cross-sectional area (cm^2), 2.3 is the conversion factor of ln and log, L is the permeability diameter, that is, the height of the sample (cm), t_1, t_2 are the start and end time (s) of the head measurement, respectively, and H_1, H_2 are the start and end of the water head, respectively.

The permeability coefficient of the grouting material was measured by the variable head permeability test method. The test data are shown in Table 1. From Table 1, it can be seen

Table 1. Permeability Coefficient of the Grouting Material (10^{-10} m/s)

grouting material	t/d			
	1	7	14	28
Grout	37.6	8.5	1.2	0.88
cement−clay−fly ash	33.8	6.5	1.4	0.96
cement−clay−fly ash (K_{12})	43.5	10.7	2.2	1.21
clay−fly ash−waste rubber particles (SiO_2)	38.6	9.4	1.7	0.92

https://dx.doi.org/10.1021/acsomega.0c01626
ACS Omega 2020, 5, 16722−16732

that the permeability coefficient of the grout gradually increased with the increase in the content of the waste rubber particles. Compared with the pure cement slurry, the grout had a lager initial permeability coefficient. However, the permeability coefficient decreased rapidly with the development of time. The final permeability coefficient of the grout was similar to that of pure cement slurry, which was approximately 1×10^{-10} m/s, indicating good impermeability. Because of the use of fly ash, a hydrolysis reaction occurred at the initial stage of the grout, which caused a relatively uniform distribution of air bubbles inside the grout, resulting in relatively large initial porosity. With the continuous production of ettringite, nanosilica oxide reacted with the hydrolysate again to form the C−S−H gel, which wrapped around the fly ash and played a role in microfilling the internal structure. As a result, the water permeability of the grout was greatly reduced, and the antipermeability of the grout was significantly improved.

According to the "Standard for Test Methods of Basic Performance of Building Mortar",[45] the osmotic pressure of the new floor crack grout was measured. In the first step, the grouting material was prepared in accordance with the requirements of the reference test piece with high impermeability. After the test piece was demolded, it was cured according to the relevant maintenance standards. After curing to the specified age, the test piece was taken out, cleaned, completely dried, and sealed into the SS-1.5-type mortar infiltrator for osmotic pressure test.

As shown in Figure 6, the osmotic pressure of the floor grouting material gradually decreased with the increase of the rubber particle content. When the rubber particle content was 20% of the total mass, the osmotic pressure of the grout was 0.8 MPa, and the impermeability reached level P6, indicating that the test piece had good impermeability.

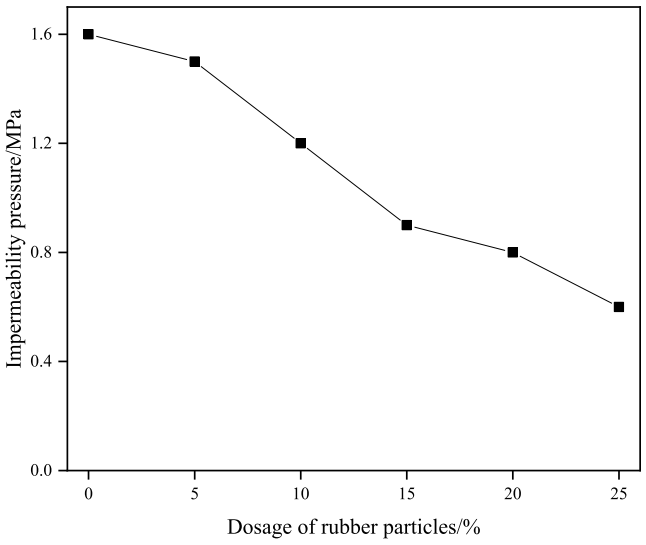

Figure 6. Effect of different rubber particle contents on osmotic pressure.

2.3. Corrosion Resistance of Grouting Stones in the Water Environment of the Mine Floor. Because of the complex formation of the coal seam floor, the chemical characteristics of the water in the floor were different under different geological conditions. The grouting material, which was used to strengthen the floor, would be in contact with the water in the floor of the mine for a long time. Therefore, it is necessary to consider the long-term stability of the grout under the mine water.

The water samples were collected from the coal mine floor of the Shandong mining area. A water sample test was carried out on the collected water sample. The acid and alkali ions contained in the water are shown in Table 2 and then poured into the container. Then, the cured grout was placed into the container and immersed for 1, 7, and 28 days until the curing period was completed.

Table 2. Hydrochemical Detection of the Coal Seam Floor

	ionic composition						
aquifer	Cation				anion		
Ordovician limestone	Ca^+	Na^+	K^+	Mg^+	HCO_3^-	SO_4^-	Cl^-

The long-term contact process of the grout with the coal seam floor water was simulated in the laboratory. The grout was placed in a container and immersed with the collected mine water samples. The ion interaction time between the grout and the mine water was determined according to the immersion duration. In the actual situation, the environment of the coal seam floor under the action of the floor water is more complicated, and it is impossible to simulate all the factors of the actual environment in the laboratory simulation; thus, the simulation for the effect of the floor water on the coal floor grouting material contained some defects. However, the laboratory simulation of the action of grout in the mine water can reflect the most important factor for the stability of the grout, that is, the chemical reaction between the internal structure of the grout and the mine water. In addition, in the laboratory, the test conditions can be well controlled, making the obtained results have high reliability. In a word, the laboratory simulation is the most effective test scheme to investigate the stability of the strengthened floor with grouting materials under the water environment in mines.[46,47]

From Figures 7 and 8, when the test pieces were immersed for 1 d, a large amount of air bubbles accumulated on the surface of the grout, and no significant change occurred on the surface of the grout. After 7d of immersion, the air bubbles on the surface of the grout were significantly reduced, and the surface of the grout slightly fell off. After 28 d, there were no obvious bubbles on the surface of the grout, and the obvious shedding was observed in the grout with a rubber content of 25%. Based on the comparison of the above pictures, it was found that there was a small amount of CaO inside the grout. After the test pieces come in contact with water, a hydration reaction occurred and caused a large number of bubbles to accumulate on the surface of the grout. After CaO reacted with water, a large amount of OH ions was released. OH ions reacted with H^+ ions in the mine water, which reduced the amount of H^+ ions in the water and led to a decrease in the acidity of the water. After 7 d, the water was changed from weakly acidic to weakly alkaline, which reduced the corrosion of grout in weakly acidic environments, and then caused the grout to enter a stable state.

2.4. Microscopic Analysis on Grouting Consolidation of the New Grouting Material. The APREO scanning electron microscope produced by the American FEI company was used to observe the grout samples. The micromorphological characteristics and pore development of each composition phase were analyzed.

https://dx.doi.org/10.1021/acsomega.0c01626
ACS Omega 2020, 5, 16722−16732

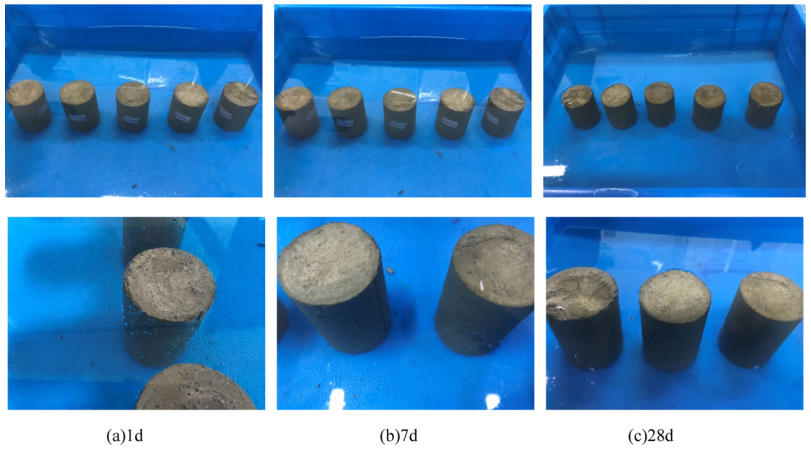

Figure 7. Soaking in mine water environment at different curing ages.

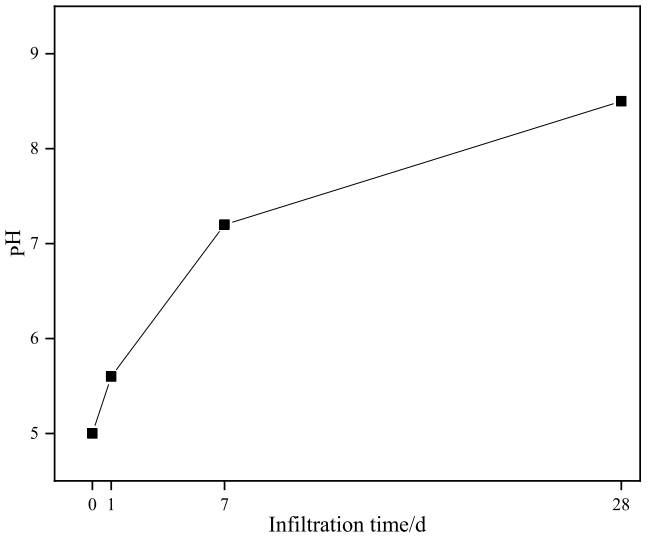

Figure 8. Change of pH value.

SEM was used to analyze the micromorphology of the grout, and then, the microcauses for the final strength of the grout were analyzed and obtained. Afterward, the 28 day old grout specimens were evaluated in the microscopic scanning test.

2.4.1. Microscopic Analysis of Different Contents of Rubber Particles. The following figures show the microstructure of the grout specimens with different contents of rubber particles.

From Figures 9 and 10, when the contents of rubber particles were 5 and 10%, the waste rubber particles inside the grout exhibited a lower degree of adhesion with other cementitious materials, and the internal particle arrangement was relatively uniform. After treatment, large irregular cracks

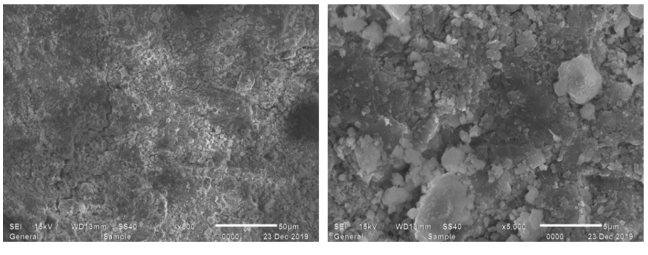

Figure 9. Microstructure of 5% grouting stones with rubber particles.

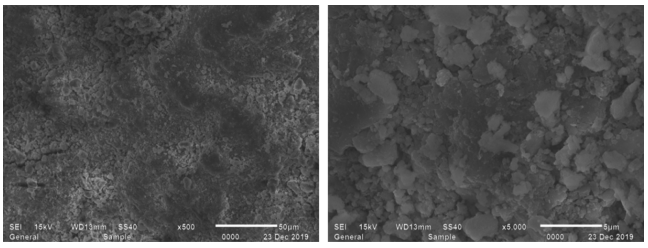

Figure 10. Microstructure of 10% grouting stones with rubber particles.

appeared around the rubber particles. It can be seen from Figures 11 and 12 that when the contents of waste rubber

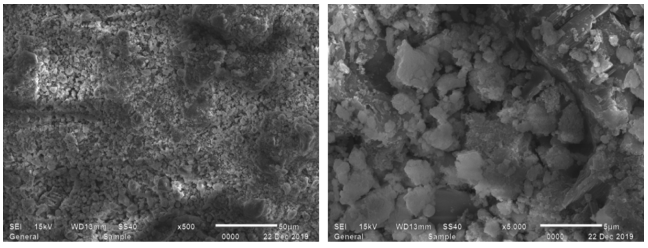

Figure 11. Microstructure of 15% grouting stones with rubber particles.

particles were 15 and 20%, the rubber particles inside the grout had good bonding with other gelling materials, the spacing between the particles was small, and a sufficient chemical reaction occurred between the cementing materials to produce a completely hydrated product, that is, ettringite, which surrounded the particles and increased the compactness of the

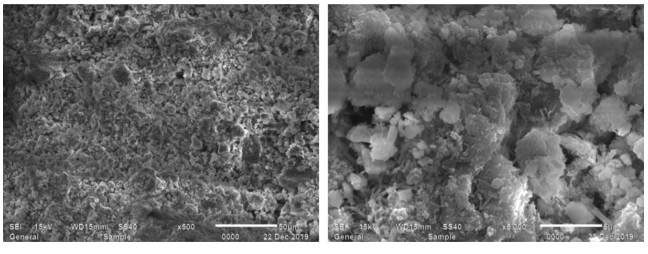

Figure 12. Microstructure of 20% grouting stones with rubber particles.

https://dx.doi.org/10.1021/acsomega.0c01626
ACS Omega 2020, 5, 16722−16732

grouting material. From Figure 13, it can be seen that when the content of waste rubber particles was 25%, the internal

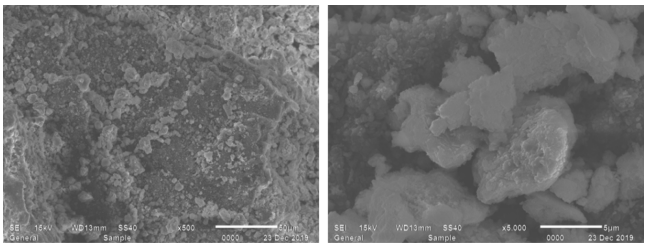

Figure 13. Microstructure of 25% grouting stones with rubber particles.

adhesion degree of the grout decreased, and peeling and adhesion phenomena began to occur. The spacing between the internal particle increased, and the combined effect of rubber particles and gelling material was reduced, which caused the peeling phenomenon. Based on the comparison of five groups of figures, the rubber particles can play a skeleton role. In addition, because of the elasticity of the rubber particles and the friction between the rubber particles and the gelling material, the shear resistance and the compressive performance of the grout can be highly improved. However, when the content of rubber particles was too high, the spacing between the particles decreased, the internal bonding capacity of the grout was decreased, and the peeling phenomenon was easy to occur. As a result, the grouting material was unable to withstand large pressure and shear force.

2.4.2. Microscopic Analysis of Different Contents of Nanosilica. The following figures show the microstructure of the grout specimens with different contents of nanosilica.

Figures 14−16 show the microstructure images of the grout with nanosilica contents of 0, 1, and 2%, respectively. From the

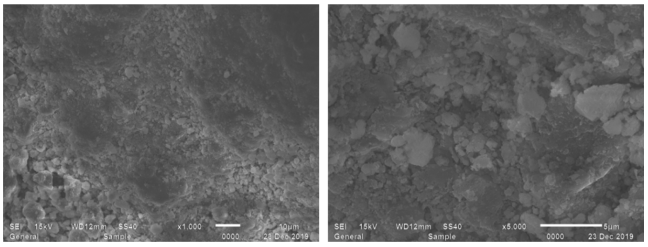

Figure 14. Microstructure of grouting stones with a nanosilica content of 0%.

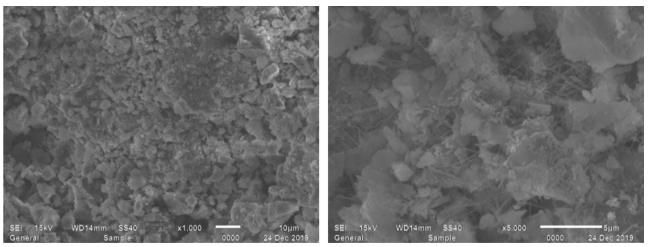

Figure 15. Microstructure of grouting stones with a nanosilica content of 1%.

figures, it can be seen that with the increase in the content of nanosilica, the internal structure of the grout became dense and the porosity was also reduced. According to the above

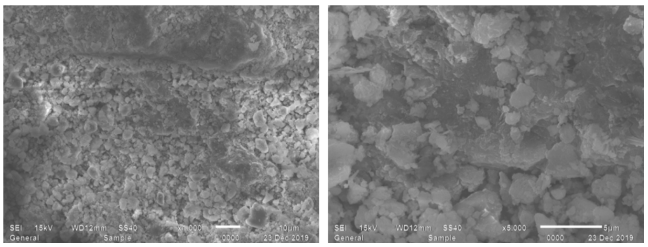

Figure 16. Microstructure of grouting stones with a nanosilica content of 2%.

images, when the content of nanosilica was 1%, the nanosilica reacted with the hydration products of fly ash to form the C−S−H gel with higher density, which surrounded the unreacted fly ash, filled the internal pores of the grout, and enhanced the compactness of the grout. When the content of nanosilica exceeded 1% of the total mass, the specific surface area of the grout was increased, resulting in an increase in water demand. As a result, the hydration degree inside the grout was greatly reduced, thereby greatly reducing both the apparent density and the strength of the grout. Therefore, considering the physical and chemical properties and the cost of the grout, the content of nanosilica is recommended to be 1% in engineering practice.

3. CONCLUSIONS

In this paper, by fully utilizing waste rubber particles and solid waste fly ash from industrial and mining enterprises, a new type of grouting material for floor reinforcement in coal seam was developed. The nanosilica was used to mix with solid waste products to develop grouting materials. The optimized ratio test, uniaxial compression test, impermeability test, and stability test under the water environment of the mine were performed. Based on the test results, supplemented by microanalysis, the following conclusions can be obtained:

(1) A new type of floor grouting and strengthening material was developed using a large amount of fly ash, waste tire rubber particles and clay as the main materials, and nanosilica as the supplement material. The developed grouting material exhibited good physical and chemical properties and microstructure. The optimal ratio of the compositions was as follows: 65% fly ash, 20% waste rubber particles, 15% clay, and 1% nanosilica. At the age of 28 days, the compressive strength was 9.7 MPa, and the osmotic pressure was 0.8 MPa, which can fully meet the requirements for the strength and impermeability of the grouting floor. Thus, the developed grouting material had high applicability and economic benefits.

(2) In the new grouting material, the optimal content of waste rubber particles was 20%. The combination of rubber particles and cementitious materials as well as the friction between the rubber particles and the inner wall of the crack can effectively improve the compression and shear stress of the grout. This can not only improve the workability of the grouting material but also benefit the strength development of the pores in the grout. The optimal content of nanosilica was 1%, which can completely react with the hydrolysate and produce the gelling materials with high density, thus improving the consolidation strength of grout.

(3) The impermeability of the grouting material was evaluated using the variable head test and the

https://dx.doi.org/10.1021/acsomega.0c01626
ACS Omega 2020, 5, 16722−16732

osmometer test. The osmotic pressure of the grouting material was measured to be as high as 0.8 MPa, and the impermeability achieved level P6, indicating that the developed grouting material exhibited good impermeability.

(4) The microscopic analysis results of the grouting materials demonstrated that when the content of waste rubber particles was 20% and the content of nanosilica was 1%, the structure was more compacted, the internal pore structure was effectively improved, and the strength in the later stage was more stabilized.

(5) In this paper, the developed grouting material for floor reinforcement based on solid waste products was evaluated in the laboratory. The corresponding proportions and performance parameters were obtained. It is necessary to verify the reinforcement effect of this newly developed grouting material in the actual application at the mine site and to further optimize the proportions of compositions through experiments.

4. MATERIALS AND METHODS

4.1. Objectives of Research and Development. When designing and developing the waste rubber particle−clay−fly ash grouting material system, the key consideration is the balance between the amount of solid waste and the material properties. The design should focus on the requirements of the grouting material properties; that is, the greater ultimate compressive strength of the material than the hydrostatic pressure of the presurge water meets the impermeability requirements of grouting reinforcement and can maintain long-term stability. After the requirements are met, the proportion of solid waste products should be increased.

4.2. Analysis on Experimental Materials. *4.2.1. Rubber Particles of Discarded Tires (R).* In the test, the waste tire rubber particles processed and produced in Lingshou County, Hebei, were used. The particle size was 1−3 mm, the apparent density was 1250 kg/m^3, the specific gravity of the rubber particles was 1.2, and the air-dry moisture content was 0. The chemical composition is shown in Table 3, and the particle morphology is shown in Figure 17.

4.2.2. Fly Ash (F). The fly ash used was the Grade I fly ash produced in a power plant in Shandong. The density of fly ash was tested to be 1.07−2.40 g/cm^3. The color of the fly ash was grayish white. The fundamental properties of fly ash used are shown in Tables 4 and 5.

From Table 4, it can be seen that the chemical composition of fly ash has the following characteristics: (1) the content of SiO_2 is about 54.14%, and the content of CaO is small, indicating that the main ingredient is quartz and the activity of the material is weak. (2) The content of Al is relatively high. The content of Al_2O_3 accounts for 25.67%, indicating that the components of fly ash are relatively stable and the content of the active minerals is low. (3) The alkalinity is low. The ratio of fly ash (CaO + MaO)/(SiO_2) is low, indicating that it is a low-alkaline mineral.

4.2.3. Clay (C). The clay used in the experiment was provided by a mine in Shandong Province with a density of about 1.40 g/cm^3. The color of the clay was dark red. The basic properties of clay are shown in Tables 6 and 7. The clay was mainly composed of SiO_2, Al_2O_3, and a small amount of Fe_2O_3.

4.2.4. Admixtures. Besides, the quicklime produced in Qingdao, Shandong Province, was used as the stimulant. The quicklime had white color and was sieved with the opening of 0.06 mm. The effective calcium oxide in the sample was determined to be 73%. The hydrophilic nanosilica produced in Qingdao, Shandong, commonly known as white carbon, was used as the consolidation agent in the test. The white carbon had a specific surface area of 148 m^2/g. The added components had a very small amount; thus, their physical and chemical properties are not explained here.

4.3. Experimental Method. The waste tire rubber particles, fly ash, and clay were mixed according to a certain ratio. After the sample was evenly mixed, the additives were added, and then, the sample was evenly mixed with water to

Table 3. Chemical Composition of Rubber Particles[a]

type	rubber hydrocarbon content	acetone extract	ash	carbon black	other oxides
PC rubber powder	45.8	18.4	4.1	26.2	5.5
PC + LC rubber powder	47.6	15.6	6.2	28.7	3.9
TB rubber powder	49.1	14.5	5.8	27.3	3.3

[a]Note: PC—passenger car tires; LT—light truck tires; and TB—truck, large passenger car tires.

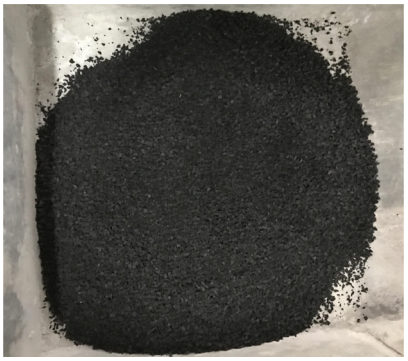

Figure 17. Rubber particles of waste tires.

Table 4. Chemical Composition of Fly Ash (Unit: %)

Al_2O_3	CaO	Fe_2O_3	ignition loss	MgO	SiO_2	SO_3
25.67	4.16	4.87	8.75	1.56	54.14	0.85

Table 6. Chemical Composition of the Clay (Unit: %)

Al_2O_3	CaO	Fe_2O_3	impurities	MgO	SiO_2	K_2O
35.38	1.96	2.04	8.34	0.34	49.86	2.08

Table 5. Fundamental Properties of the Fly Ash Used

density (g/cm^3)	bulk density (g/cm^3)	specific surface area (cm^2/g)	45 μm square hole sieve residue/%	water demand ratio/%	28 d compressive strength ratio%
1.07−2.40	1.0−1.3	1500−5000	≤12	≤95	37−85

https://dx.doi.org/10.1021/acsomega.0c01626
ACS Omega 2020, 5, 16722−16732

Table 7. Fundamental Properties of the Clay Used

moisture content/%	proportion	density (g/cm^3)	pore ratio	plastic limit/%	liquid limit/%	plastic limit index/%	liquid limit index/%	undrained shear strength index	
								cohesion (KPa)	internal friction angle (deg)
74.1	2.72	1.40	2.07	28.4	55.5	27.1	1.68	17	18

Table 8. Composition Ratio of Test Materials[a]

level	influencing factors		
	water−cement ratio	cement ratio (R/C)%	nanosilica content/%
1	0.7	0:35	0
2		5:30	
3		10:25	1
4		15:20	
5		20:15	2
6		25:10	

[a]Note: nanosilica content is the total mass percentage of solids.

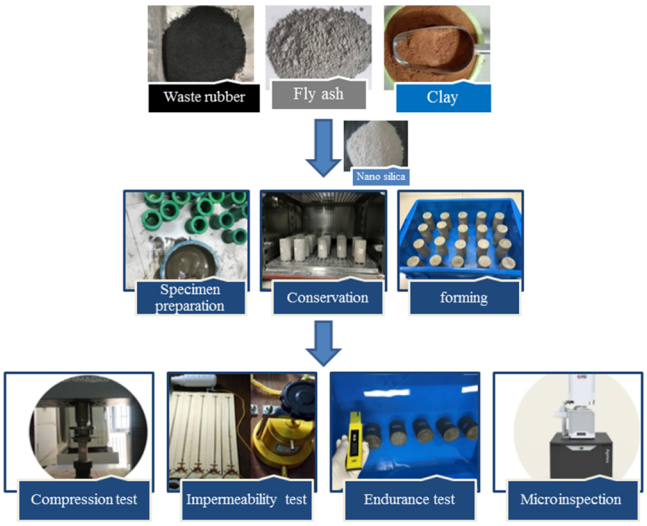

Figure 18. Experimental process.

prepare a grout body. The grout was cured for 3, 7, and 28 days, during which the performance tests including the physical and mechanical property test, stability test in the mine water environment, and microanalysis test were conducted, respectively.

4.4. Experimental Design. The proportion of grouting materials was not only designed to meet the strengthening requirements of grouting in coal seam floor but also aimed to take full use of the waste rubber particles and industrial waste fly ash to obtain a new type of flooring strengthening filler with superior performance, low cost, and strong applicability. Comprehensively considering the influencing factors, a series of experiments were designed to analyze the physical and chemical characteristics of the new grouting material, which included a total of six levels and two factors, that is, the cement content and the nanosilica content. The contents of the materials are shown in Table 8, and the experimental process is shown in Figure 18.

AUTHOR INFORMATION

Corresponding Authors

Qi Zhang − *Department of Civil and Environmental Engineering, Stanford University, Stanford 94306, California, United States;* orcid.org/0000-0002-4637-6308; Email: qzhang94@stanford.edu

Wenquan Zhang − *College of Mining and Safety Engineering, State Key Laboratory of Mine Disaster Prevention and Control, and National Demonstration Center for Experimental Mining Engineering Education, Shandong University of Science and Technology, Qingdao 266590, China;* Email: wenquanzhang415@163.com

Authors

Xianxiang Zhu − *College of Mining and Safety Engineering, State Key Laboratory of Mine Disaster Prevention and Control, and National Demonstration Center for Experimental Mining Engineering Education, Shandong University of Science and Technology, Qingdao 266590, China;* orcid.org/0000-0002-4112-8436

Jianli Shao − *College of Mining and Safety Engineering, State Key Laboratory of Mine Disaster Prevention and Control, and National Demonstration Center for Experimental Mining Engineering Education, Shandong University of Science and Technology, Qingdao 266590, China*

Zaiyong Wang − *College of Mining and Safety Engineering, State Key Laboratory of Mine Disaster Prevention and Control, and National Demonstration Center for Experimental Mining Engineering Education, Shandong University of Science and Technology, Qingdao 266590, China*

Xintao Wu − *College of Mining and Safety Engineering, State Key Laboratory of Mine Disaster Prevention and Control, and National Demonstration Center for Experimental Mining Engineering Education, Shandong University of Science and Technology, Qingdao 266590, China*

Complete contact information is available at: https://pubs.acs.org/10.1021/acsomega.0c01626

Notes

The authors declare no competing financial interest.

ACKNOWLEDGMENTS

The authors are grateful to the National Natural Science Foundation of China (51774199) and the Natural Science Foundation of Shandong Province for the support of major basic research projects (ZR2018ZC0740).

REFERENCES

(1) Jalal, M.; Nassir, N.; Jalal, H. Waste tire rubber and pozzolans in concrete: a trade-off between cleaner production and mechanical properties in a greener concrete. *J. Clean. Prod.* **2019**, *238*, 117882.

(2) Su, H.; Yang, J.; Ling, T.-C.; Ghataora, G. S.; Dirar, S. Properties of concrete prepared with waste tyre rubber particles of uniform and varying sizes. *J. Clean. Prod.* **2015**, *91*, 288−296.

(3) Yu, K.; Wang, H.; Han, H.; Li, R.; Liu, S. Hydrogen peroxide oxidizing modification of crumb tire rubber and its application in modified bitumen. *J. Tianjin Univ.* **2014**, *47*, 949−954.

(4) Blinova, I.; Bityukova, L.; Kasemets, K.; Ivask, A.; Käkinen, A.; Kurvet, I.; Bondarenko, O.; Kanarbik, L.; Sihtmäe, M.; Aruoja, V.; Schvede, H.; Kahru, A. Environmental hazard of oil shale combustion fly ash. *J. Hazard. Mater.* **2012**, *229−230*, 192−200.

(5) Jambhulkar, H. P.; Shaikh, S. M. S.; Kumar, M. S. Fly ash toxicity, emerging issues and possible implications for its exploitation in agriculture; Indian scenario: A review. *Chemosphere* **2018**, *213*, 333−344.
(6) Yan, K.; Li, L.; Zheng, K.; Ge, D. Research on properties of bitumen mortar containing municipal solid waste incineration fly ash. *Constr. Build. Mater.* **2019**, *218*, 657−666.
(7) Zhang, X.; Saha, P.; Cao, L.; Li, H.; Kim, J. Devulcanization of waste rubber powder using thiobisphenols as novel reclaiming agent. *Waste Manag.* **2018**, *78*, 980−991.
(8) Migas, P.; Zukowski, W.; Baron, J.; Wrona, J. Cenospheric and sand fluidized bed as an environment for waste rubber combustion-comparisons of decomposition dynamics and flue gas emission. *Therm. Sci.* **2019**, *23*, 1217−1229.
(9) Khordehbinan, M.; Kaymanesh, M. R. Chemical analysis and middle-low temperature functional of waste polybutadiene rubber polymer modified bitumen. *Pet. Sci. Technol.* **2020**, *38*, 8−17.
(10) Xiang, H. P.; Qian, H. J.; Lu, Z. Y.; Rong, M. Z.; Zhang, M. Q. Crack healing and reclaiming of vulcanized rubber by triggering the rearrangement of inherent sulfur crosslinked networks. *Green Chem.* **2015**, *17*, 4315.
(11) Aliakbari, M.; Jazani, O. M.; Sohrabian, M. Epoxy adhesives toughened with waste tire powder, nanoclay, and phenolic resin for metal-polymer lap joint applications. *Prog. Org. Coating* **2019**, *136*, 105291.
(12) Gupta, T.; Siddique, S.; Sharma, R. K.; Chaudhary, S. Behaviour of waste rubber powder and hybrid rubber concrete in aggressive environment. *Constr. Build. Mater.* **2019**, *217*, 283−291.
(13) He, T.; Xu, R.; Da, Y.; Yang, R.; Chen, C.; Liu, Y. Experimental study of high-performance autoclaved aerated concrete produced with recycled wood fibre and rubber powder. *J. Clean. Prod.* **2019**, *234*, 559−567.
(14) Gualtieri, M.; Andrioletti, M.; Vismara, C.; Milani, M.; Camatini, M. Toxicity of tire debris leachates. *Environ. Int.* **2005**, *31*, 723−730.
(15) Kardos, A. J.; Durham, S. A. Strength, durability, and environmental properties of concrete utilizing recycled tire particles for pavement applications. *Constr. Build. Mater.* **2015**, *98*, 832−845.
(16) Mittal, R. K.; Gill, G. Sustainable application of waste tire chips and geogrid for improving load carrying capacity of granular soils. *J. Clean. Prod.* **2018**, *200*, 542−551.
(17) Abbaspour, M.; Aflaki, E.; Moghadas Nejad, F. Reuse of waste tire textile fibers as soil reinforcement. *J. Clean. Prod.* **2019**, *207*, 1059−1071.
(18) Bekhiti, M.; Trouzine, H.; Rabehi, M. Influence of waste tire rubber fibers on swelling behavior, unconfined compressive strength and ductility of cement stabilized bentonite clay soil. *Constr. Build. Mater.* **2019**, *208*, 304−313.
(19) Hidalgo Signes, C.; Garzón-Roca, J.; Martínez Fernández, P.; Garrido de la Torre, M. E.; Insa Franco, R. Swelling potential reduction of Spanish argillaceous marlstone Facies Tap soil through the addition of crumb rubber particles from scrap tyres. *Appl. Clay Sci.* **2016**, *132*−*133*, 768−773.
(20) Li, Y.; Zhang, S.; Wang, R.; Dang, F. Potential use of waste tire rubber as aggregate in cement concrete-A comprehensive review. *Constr. Build. Mater.* **2019**, *225*, 1183−1201.
(21) Medina, N. F.; Garcia, R.; Hajirasouliha, I.; Pilakoutas, K.; Guadagnini, M.; Raffoul, S. Composites with recycled rubber aggregates: Properties and opportunities in construction. *Constr. Build. Mater.* **2018**, *188*, 884−897.
(22) Xin, L.; Liu, H. L.; Shen, Y.; He, J. Consolidated undrained triaxial compression tests on lightweight soil mixed with rubber chips of scrap tires. *Chin. J. Geotech. Eng.* **2010**, *32*, 428−433.
(23) Xin, L.; Liu, H. L.; Shen, Y.; He, J. Unconfined compressive test of lightweight soil mixed with rubber chips of scrap tires. *J. PLA Univ. Technol. Sci.* **2010**, *11*, 79−83.
(24) Liu, F. C.; Wu, M. T.; Wang, H. D. Microscopic Study on Mechanical Behavior of Granulated Waste Tires and Sand Mixture under Biaxial Compression Conditions. *Chin. J. Undergr. Space Eng.* **2019**, *15*, 1055−1065.
(25) Liu, F. C.; Wu, M. T.; Wang, H. D. Effect of particle size ratio and mix ratio on mechanical behavior of rubber-sand mixtures. *J. Eng. Geol.* **2019**, *27*, 376−389.
(26) Feng, Z.-g.; Rao, W.-y.; Chen, C.; Tian, B.; Li, X.-j.; Li, P.-l.; Guo, Q.-l. Performance evaluation of bitumen modified with pyrolysis carbon black made from waste tyres. *Constr. Build. Mater.* **2016**, *111*, 495−501.
(27) Gupta, V. K.; Ganjali, M. R.; Nayak, A.; Bhushan, B.; Agarwal, S. Enhanced heavy metals removal and recovery by mesoporous adsorbent prepared from waste rubber tire. *Chem. Eng. J.* **2012**, *197*, 330−342.
(28) Cazan, C.; Cosnita, M.; Duta, A. Effect of PET functionalization in composites of rubber−PET−HDPE type. *Arabian J. Chem.* **2017**, *10*, 300−312.
(29) Li, C. Y.; Liu, H. B.; Wei, H. B. Experimental research on dynamic characteristics of fly ash soil improved by rubber particles. *Rock Soil Mech.* **2011**, *32*, 2025.
(30) Aslani, F.; Sun, J.; Huang, G. Mechanical Behavior of Fiber-Reinforced Self-Compacting Rubberized Concrete Exposed to Elevated Temperatures. *J. Mater. Civ. Eng.* **2019**, *31*, 04019302.
(31) Aly, A. M.; El-Feky, M. S.; Kohail, M.; Nasr, E.-S. A. R. Performance of geopolymer concrete containing recycled rubber. *Constr. Build. Mater.* **2019**, *207*, 136−144.
(32) Lo Presti, D.; Fecarotti, C.; Clare, A. T.; Airey, G. Toward more realistic viscosity measurements of tyre rubber−bitumen blends. *Constr. Build. Mater.* **2014**, *67*, 270−278.
(33) Sun, Q.; Tian, S.; Sun, Q.; Li, B.; Cai, C.; Xia, Y.; Wei, X.; Mu, Q. Preparation and microstructure of fly ash geopolymer paste backfill material. *J. Clean. Prod.* **2019**, *225*, 376−390.
(34) Lee, Y.-R.; Soe, J. T.; Zhang, S.; Ahn, J.-W.; Park, M. B.; Ahn, W.-S. Synthesis of nanoporous materials via recycling coal fly ash and other solid wastes: A mini review. *Chem. Eng. J.* **2017**, *317*, 821−843.
(35) Chen, L. Y.; Wang, S. Research and application of fly ash grouting material. *J. Chengdu Univ. Technol., Sci. Technol. Ed.* **2007**, *02*, 206−209.
(36) Wan, Z. *Experimental Investigation on Anti-Seepage Reinforcement Effect of Fracture Grouting in the Yellow River Embankment*; Shandong University: Jinan, 2019.
(37) Zhang, W.; Zhu, X.; Xu, S.; Wang, Z.; Li, W. Experimental study on properties of a new type of grouting material for the reinforcement of fractured seam floor. *J. Mater. Res. Technol.* **2019**, *8*, 5271−5282.
(38) Han, W.; Li, G.; Sun, Z.; Luan, H.; Liu, C.; Wu, X. Numerical Investigation of a Foundation Pit Supported by a Composite Soil Nailing Structure. *Symmetry* **2020**, *12*, 252.
(39) Wang, C.; Jiang, Y.; Liu, R.; Wang, C.; Zhang, Z.; Sugimoto, S. Experimental Study of the Nonlinear Flow Characteristics of Fluid in 3D Rough-Walled Fractures During Shear Process. *Rock Mech. Rock Eng.* **2020**, *53*, 2581.
(40) Ren, D.; Zhou, D.; Liu, D.; Dong, F.; Ma, S.; Huang, H. Huang H. Formation mechanism of the Upper Triassic Yanchang Formation tight sandstone reservoir in Ordos Basin—Take Chang 6 reservoir in Jiyuan oil field as an example. *J. Pet. Sci. Eng.* **2019**, *178*, 497−505.
(41) Shi, Z.; Wang, Q.; Xu, L. Experimental Study of Cement Alkali-Resistant Glass Fiber (C-ARGF) Grouting. *Materials* **2020**, *13*, 605.
(42) Huang, H.; Babadagli, T.; Chen, X.; Li, H.; Zhang, Y. Performance Comparison of Novel Chemical Agents for Mitigating Water-Blocking Problem in Tight Gas Sandstones. *SPE Reservoir Eval. Eng.* **2020**, 1−9.
(43) Shang, H. X. *Research on the Deformation and Seepage of Grouting Fractured Rock Mass*; WuHan Polytechnic University: Wuhan, 2017.
(44) Zhang, Q.; Choo, J.; Borja, R. I. On the preferential flow patterns induced by transverse isotropy and non-Darcy flow in double porosity media. *Comput. Methods. Appl. Mech. Eng.* **2019**, *353*, 570−592.

https://dx.doi.org/10.1021/acsomega.0c01626
ACS Omega 2020, 5, 16722−16732

(45) JGJ/T70-2009, Standard for test method of performance on building mortar(S).
(46) Qin, J.; Cui, X.; Yan, H.; Lu, W.; Lin, C. Active treatment of acidic mine water to minimize environmental impacts in a densely populated downstream area. *J. Clean. Prod.* **2018**, *210*, 309−316.
(47) Chen, S. J.; Du, Z. W.; Zhang, Z.; Zhang, H. W.; Xia, Z. G.; Feng, F. Effects of chloride on the early mechanical properties and microstructure of gangue-cemented paste backfill. *Constr. Build. Mater.* **2020**, *235*, 117504.

https://dx.doi.org/10.1021/acsomega.0c01626
ACS Omega 2020, 5, 16722−16732